Received: 30 September 2022 | Revised: 14 March 2023 | Accepted: 17 April 2023

DOI: 10.1002/wrna.1792

ADVANCED REVIEW

WIREs RNA WILEY

Translation machinery captured in motion

Hassan Zafar | **Ahmed H. Hassan** | **Gabriel Demo**

Central European Institute of Technology, Masaryk University, Brno, Czech Republic

Correspondence
Gabriel Demo, Central European Institute of Technology, Masaryk University, Brno, Czech Republic.
Email: gabriel.demo@ceitec.muni.cz

Funding information
Ministerstvo Školství, Mládeže a Tělovýchovy, Grant/Award Numbers: ERC_CZ/LL2008, EXCELES/LX22NPO5103

Edited by: Purusharth Rajyaguru, Associate Editor and Jeff Wilusz, Editor-in-Chief

Abstract

Translation accuracy is one of the most critical factors for protein synthesis. It is regulated by the ribosome and its dynamic behavior, along with translation factors that direct ribosome rearrangements to make translation a uniform process. Earlier structural studies of the ribosome complex with arrested translation factors laid the foundation for an understanding of ribosome dynamics and the translation process as such. Recent technological advances in time-resolved and ensemble cryo-EM have made it possible to study translation in real time at high resolution. These methods provided a detailed view of translation in bacteria for all three phases: initiation, elongation, and termination. In this review, we focus on translation factors (in some cases GTP activation) and their ability to monitor and respond to ribosome organization to enable efficient and accurate translation.

This article is categorized under:

Translation > Ribosome Structure/Function

Translation > Mechanisms

KEYWORDS

cryoelectron microscopy, structural biology, translation

1 | INTRODUCTION

The translational process in bacteria leads to protein synthesis, and it is one of the most important physiological processes in these organisms (Hershey et al., 2012). Translation is the final phase of gene expression, in which the sequence of nucleotides on the messenger RNA (mRNA) is decoded by aminoacylated transfer RNAs (tRNAs) into amino acids to form a polypeptide chain (Rodnina, 2018). This biosynthetic process occurs in a large macromolecular ribonucleoprotein complex called a ribosome (Laursen et al., 2005). The bacterial 70S ribosome consists of two subunits: the large 50S and small 30S subunit. The 30S subunit is composed of 16S ribosomal RNA (rRNA) and 21 ribosomal proteins (r-proteins), and plays a pivotal role in mRNA decoding and translation fidelity (Kaczanowska & Ryden-Aulin, 2007). The 50S subunit contains 23S and 5S rRNAs, 34 r-proteins, and the peptidyl-transferase center (PTC), where the synthesis of the polypeptide chain takes place (Byrgazov et al., 2013).

Fundamentally, translation includes four major steps, (i) initiation, (ii) elongation, (iii) termination, and (iv) recycling of the ribosome (Rodnina, 2018). In each step, there is a close collaboration between the ribosome and the appropriate tRNA or translation factors. These substrates are either rejected or accepted by the ribosome, while still maintaining the open reading frame of the mRNA.

The interactions between the mRNA and tRNA are governed by nucleic acid complementarity (Ramakrishnan, 2002). The nascent mRNA contains the message for translation encoded in the form of three nucleotides, called codons, which base-pair with the three nucleotides (anticodons) in the anticodon stem loop (ASL) of the tRNA carrying the respective amino acid (Ou et al., 2019). The process of translation largely depends upon the conformational dynamics of the ribosome (Frank & Agrawal, 2000; Ratje et al., 2010). Extensive ribosome rearrangements enable the translocation of the mRNA and tRNA during protein synthesis within the aminoacyl (A), peptidyl (P), and exit (E) sites on the mRNA programmed ribosome (Frank et al., 2007), as validated by Foster Resonance Energy Transfer (FRET) studies (Belardinelli et al., 2016; Cornish et al., 2008; Guo & Noller, 2012; Wasserman et al., 2016). These rearrangements contain a rotation (∼10°) of the 30S relative to the 50S subunit, which is also known as "intersubunit rotation," (Frank & Agrawal, 2000) and an ∼20° rotation of the head relative to the body of the 30S subunit (known as head swivel) (Ratje et al., 2010) (Figure 1). The peptidyl transfer occurs from the peptidyl-tRNA onto the aminoacyl-tRNA (aa-tRNA) following the GTP-(guanosine-5′-triphosphate) catalyzed delivery of the aa-tRNA into the A-site of the ribosome, which is mediated by elongation factor Tu (EF-Tu) as part of the ternary complex. During this process, the 30S undergoes a counterclockwise rotation, and the acceptor arm of the tRNA moves onto the 50S subunit (Frank & Gonzalez, 2010). This movement results in a rotated ribosome, in which the tRNA is in a hybrid state (A/P state). In this A/P state, the A-site of the 30S subunit is still occupied by the ASL of the tRNA, and the acceptor arm of the tRNA is present in the P-site of the 50S subunit. The translocation step proceeds when the GTP-bound elongation factor G (EF-G) initiates a clockwise (reverse) rotation (Noller et al., 2017), which enables the transfer of the ASLs of the A- and P-site tRNAs to the P- and E-sites, respectively. During reverse rotation, the head of the 30S subunit undergoes a forward head swivel that enables full accommodation of tRNAs relative to the body of the 30S subunit. This movement completes the translocation cycle, generating a non-rotated conformation of the ribosome ready for the next translocation event.

Previous structural studies mainly reported single-state structures, and most of them relied on the usage of inhibitors (Fischer et al., 2015; Gao et al., 2009; Lancaster et al., 2013; Schmeing et al., 2009), mutations (Fislage et al., 2018; Lin et al., 2015; Santos et al., 2013), or GTP analogs (Allen et al., 2005; Loveland et al., 2017; Simonetti et al., 2013) to visualize these stalled ribosome complexes with the respective translation factors. Although these structures largely contributed to the current understanding of bacterial translation, they lack some important information about critical transient conformations necessary for translation regulation and fidelity. Structural information on intermediate states of the translational apparatus with authentic substrates would unveil key details of how the ribosome and translation factors regulate each step of translation.

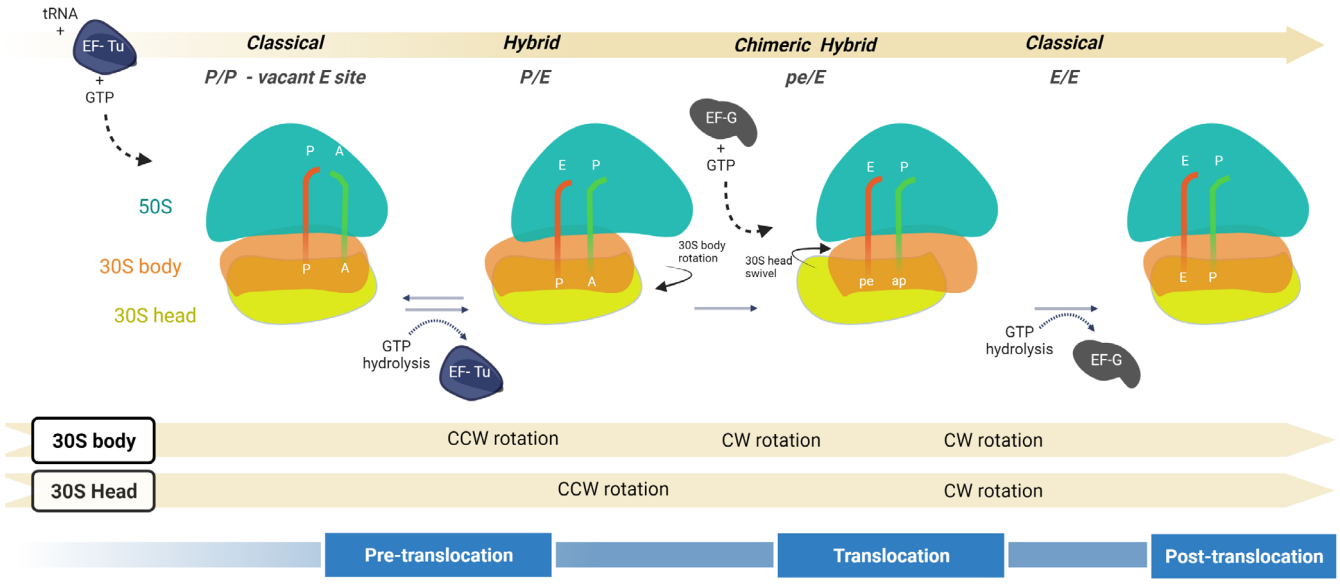

FIGURE 1 Translocation cycle scheme. The EF-Tu.GTP-catalyzed delivery of the aa-tRNA into the ribosome initiates the peptidyl transfer and rearranges the classical (pre-translocation) non-rotated ribosome with P/P, A/A tRNAs and a vacant E-site into a rotated ribosome (counterclockwise rotation of 30S subunit) with tRNAs in P/E and A/P hybrid states. During EF-G.GTP-catalyzed translocation, tRNAs are found in chimeric pe/E and ap/P hybrid states, which is accompanied by counterclockwise rotation of the 30S head. The dissociation of EF-G results in a classical (post-translocation) non-rotated ribosome containing E/E and P/P tRNAs.

Over the past two decades, cryo-electron microscopy (cryo-EM) has become the preferred method of choice for structural biologists to visualize the structures of macromolecules and/or macromolecular complexes (Earl et al., 2017; Nogales, 2016). Some of the technical advancements in this field include, (i) improved instrumentation in the sample preparation for vitrification and controlling ice thickness (Weissenberger et al., 2021), (ii) automated data collection strategies, (iii) the development of packages for image analysis (Scheres, 2012; Tang et al., 2007), (iv) beam-induced motion correction (Brilot et al., 2012; Zheng et al., 2017), and (v) improved computational approaches (Grigorieff, 2016; Punjani et al., 2017; Zivanov et al., 2018).

These advancements have enabled scientists to elucidate an ensemble of conformational states of macromolecules in a single solution at near-atomic resolution. Numerous biochemical reactions (e.g., the addition of ligands to enzymes or mixing components of macromolecular machinery) can initiate changes in conformational states (Carbone et al., 2021; Fu et al., 2019; Kaledhonkar et al., 2019; Loveland et al., 2020). These transient changes can be trapped by vitrification at specific time points and visualized by ensemble or time-resolved cryo-EM. In these specific studies, rapid freezing stops the biological reaction at one or multiple time points. However, imaging snapshots of such fast reactions requires mixing, carrying out individual reactions, and depositing the end products on the grid rapidly but in a controlled manner (Dandey et al., 2020; Frank, 2017).

Recent ensemble and time-resolved cryo-EM studies (Carbone et al., 2021; Fu et al., 2019; Kaledhonkar et al., 2019; Loveland et al., 2020) of bacterial translation enabled the depiction of all the main phases of translation in relation to ribosome dynamics and translation factor activation (e.g., GTP hydrolysis). The combination of recent structural studies in tandem with previous structural (Allen et al., 2005; Horan & Noller, 2007; Laurberg et al., 2008; Myasnikov et al., 2005; Schmeing et al., 2009; Weixlbaumer et al., 2008), biophysical (Ermolenko et al., 2007; Liu et al., 2015; Marshall et al., 2009; Trappl & Joseph, 2016) and biochemical (Goyal et al., 2015; Ieong et al., 2016; Indrisiunaite et al., 2015) studies shows the whole translation machinery in motion and describes in detail the precise and compelling nature of translation.

This review will focus on the role and advantages of ensemble or time-resolved cryo-EM in deciphering the different stages of translation in bacteria. We will describe resolved structures of the various complexes with initiation, elongation, and termination factors. At the end, we will discuss future perspectives in the field of translation, and ensemble and time-resolved cryo-EM.

2 | INITIATION

The initiation step of translation starts when the ribosome recruits an mRNA followed by the selection of the open reading frame (ORF) (Samatova et al., 2020). To efficiently establish the protein synthesis, an AUG initiation codon and a Shine–Dalgarno (SD) sequence should be present on the mRNA (Shine & Dalgarno, 1974). The SD sequence is complementary to the 3′-end anti-SD sequence of 16S rRNA of the 30S subunit (Steitz & Jakes, 1975). Initially, the mRNA with the translation initiation region and initiator fMet-tRNA^{fMet} bind in the P-site of the 30S subunit with the assistance of initiation factors (IFs) (Milon et al., 2012). The 30S initiation complex (30S IC) is fully formed when the codon-anticodon pairing is established by the ASL of the initiator fMet-tRNA^{fMet} and the AUG start codon. The next phase includes the association of the 30S IC with the 50S subunit, resulting in the formation of a 70S initiation complex (70S IC) (Marshall et al., 2009; Milon et al., 2008). GTP hydrolysis and dissociation of the IFs ensure the generation of the elongation-capable 70S complex (70S EC) to enable the formation of a dipeptide with the subsequent aa-tRNA encoded by the second mRNA codon.

In bacteria, three IFs—IF1, IF2, and IF3—are important players in the initiation step of translation. These IFs regulate the speed and accuracy of the initiation process (Antoun et al., 2006a, 2006b). The binding of IF1 to the A-site of the 30S subunit is known to bridge both IF2 and IF3 to enhance their activities (Julian et al., 2011; Simonetti et al., 2008). IF2 is a GTPase that binds the initiator fMet-tRNA^{fMet} and guides it correctly to the P-site of the 30S IC. During binding with the fMet-tRNA^{fMet}, the orientation of the IF2 enables a suitable conformation for its C-2 domain to bind the formyl-methionyl moiety and catalyze a GTP-dependent ribosomal subunit association (Antoun et al., 2003; Goyal et al., 2015; Grigoriadou, Marzi, Pan, et al., 2007; Marshall et al., 2009). IF3 is important for accurate selection of the initiator fMet-tRNA^{fMet} (Grigoriadou, Marzi, Pan, et al., 2007). Prior to the formation of 70S IC, the N-terminal domain (NTD) and C-terminal domain (CTD) of IF3 occupy the E- and P-sites, respectively, on the 30S subunit along the mRNA path, and prevent the binding of the 50S subunit (Hussain et al., 2016; McCutcheon et al., 1999).

Past structural studies of the 30S IC (Julian et al., 2011; Simonetti et al., 2008; Simonetti et al., 2013) and 70S IC (Allen et al., 2005; Myasnikov et al., 2005; Simonetti et al., 2013; Sprink et al., 2016) revealed that the process of initiation could be highly dynamic, with ribosomal subunits, IFs, and initiator fMet-tRNA^{fMet} found in a variety of different conformational states. For example, some studies indicated that IF2 may undergo substantial conformational changes during GTP hydrolysis, which would assist the formation of the 70S IC (Allen et al., 2005; Myasnikov et al., 2005). Although several biochemical and biophysical studies indicated the timing of IFs dissociation (Antoun et al., 2003; Goyal et al., 2015; Milon et al., 2008) and ribosomal subunit association catalyzed by GTP hydrolysis (Goyal et al., 2015; Grigoriadou, Marzi, Pan, et al., 2007; Marshall et al., 2009), it has been challenging to postulate a broadly accepted structural mechanism for translation initiation in combination with structural knowledge. The discrepancies arose from several intermediate structures of translation initiation with contradictory dynamics for ribosome rotation and initiator fMet-tRNA^{fMet} positioning. Therefore, the main unanswered question was how the IFs dynamically cooperate with the 30S subunit and 70S ribosome to select the correct initiator tRNA to translate the message.

Recent ensemble cryo-EM revealed a dynamic equilibrium of multiple conformations for IF3 and the 30S subunit during the formation of 30S IC in the presence or absence of IF2 (Hussain et al., 2016) (Figure 2a). The reported structural conformations of IF3 during fMet-tRNA^{fMet} selection and accommodation were also identified by single-molecule FRET (smFRET) study (Elvekrog & Gonzalez, 2013). When the fMet-tRNA^{fMet} is absent, the CTD of IF3 remains localized near the P-site of the 30S subunit shielding the AUG start codon, thereby precluding the fMet-tRNA^{fMet} from forming the Watson-Crick base pairing. The IF1 occupies the A-site on the 30S subunit and provides an anchoring platform for IF3 to stabilize the IF3-CTD to discriminate the fMet-tRNA^{fMet}. The 30S subunit is observed in "open" and "closed" conformations as the head of 30S moves away or closer to the body of 30S (Hussain et al., 2016; Korostelev, 2022). This movement (head tilt) regulates the opening (widening or narrowing) of the mRNA tunnel from the A-site to the P-site by more than ~10 Å. In the initial step of fMet-tRNA^{fMet} binding, the 30S is in its open conformation. The widened P-site is predisposed to accommodate the fMet-tRNA^{fMet}, since G1338 and A1339 of 16S rRNA are exposed and positioned to interact with highly conserved G-C base pairs in the ASL of the tRNA. During the accommodation of the ASL into the P-site, the CTD of IF3 slightly shifts from the P-site while preserving some interactions with IF1. At full ASL accommodation and Watson–Crick base pairing with the AUG codon, the fMet-tRNA^{fMet} is stabilized by the closed conformation of the 30S subunit and the CTD of IF3 dissociates from the P-site.

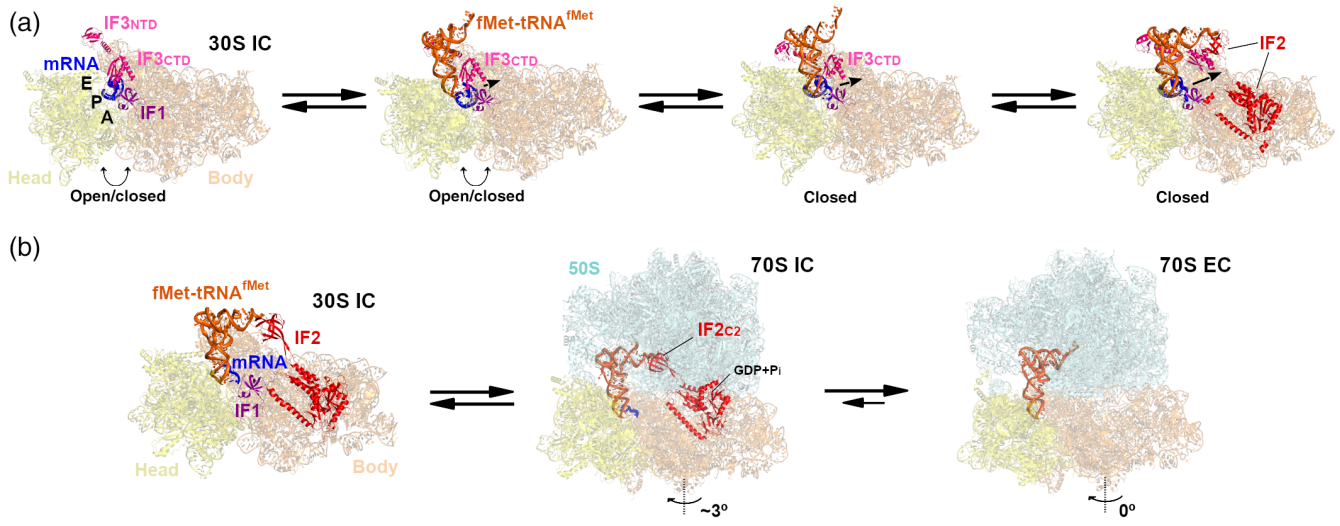

FIGURE 2 Structure-based view of conformational dynamics of initiation factors and ribosome (30S subunit) defining the bacterial translation initiation reaction. (a) Cryo-EM ensemble trajectory of 30S IC complex formation proposing "mRNA binds before tRNA" pathway (Hussain et al., 2016). The double-ended curved arrows highlight the possible head tilt movement that generates open or closed conformations of the 30S subunit. The single arrow indicates the multiple conformations (dissociation) of the C-terminal domain of IF3 during the formation of 30S IC and fMet-tRNA^{fMet} accommodation. (b) Time-resolved cryo-EM trajectory of late steps of bacterial translation initiation (Kaledhonkar et al., 2019). The formation of 70S IC initiates rapid GTP hydrolysis and IF1 dissociation. The semi-rotated 70S IC matures into 70S EC with the release of Pi from IF2 and dissociation of IF2 in GDP-bound form. The curved arrows highlight the 30S body rotation that generates semi-rotated 70S IC or non-rotated 70S EC.

A time-resolved cryo-EM, using the mixing-spraying approach (Chen et al., 2015; Fu et al., 2016), helped to visualize IF2 bound to 30S and 70S ICs in the GTP-catalyzed reaction (Kaledhonkar et al., 2019) (Figure 2b). When comparing the 30S IC to 70S IC, the IF2 exhibits different conformational states, indicating that the formation of 70S IC is dependent on IF2. At the ≤80 ms time point, the 70S IC was populated at the maximum level, revealing early IF1 dissociation to enable the formation of inter-subunit bridge B2a (crucial for subunit association) and conformational freedom for IF2. Specifically, the C-2 domain of IF2 in 70S IC is ~10 Å closer to the 30S subunit, which enables the subunits to join and selectively stabilize the 70S IC in a semi-rotated state. Moreover, the IF2 was captured in a native GDP.Pi form on the 70S IC. Therefore, the obtained structure sheds more light on the time scale of the ribosome and IF2 conformational dynamics and GTP hydrolysis. First, the rate of Pi release from IF2 is slower than the rate of IF2 dissociation (Goyal et al., 2015; Grigoriadou, Marzi, Kirillov, et al., 2007), thus the 70S IC structure suggests that IF2 may not undergo immediate conformational changes during the GTP hydrolysis. These late IF2 conformational changes are regulated by Pi release and/or GDP release from IF2 to initiate the IF2 dissociation (Basu et al., 2022). The IF2 dissociation enables the generation of a non-rotated ribosome capable of elongation, and simultaneously shifts the 3′ CAA-fMet end of fMet-tRNA^{fMet} by ~25 Å to a peptidyl/peptidyl (P/P) configuration in the PTC of the 50S subunit.

Taken together, these structural studies provide a structure-based time-ordered view of how a series of conformational changes in initiation factors and ribosome (30S subunit), fMet-tRNA^{fMet} positioning, and GTP hydrolysis determine the translation initiation reaction pathway to generate a 70S elongation-capable complex. However, several questions regarding the initiation pathway still remain open for investigation. For example, (i) does the IF1 binding occur in the early stages of 30S IC formation to help IF3 discriminate against other tRNAs, or (ii) what IF2-dependent events initiate IF1 release?

3 | ELONGATION

The elongation process involves repetitive decoding cycles, peptide bond formation and translocation (reviewed in Ling & Ermolenko, 2016; Noller et al., 2017; Ogle & Ramakrishnan, 2005; Prabhakar et al., 2019; Rodnina, 2018). First, the elongation occurs as the second codon (in the A-site of the ribosome) next to the start codon is recognized and decoded by the cognate aa-tRNA. Next, a peptide bond is formed within the PTC of the ribosome between the peptidyl-tRNA and aa-tRNA. After the formation of the peptide bond, the rotated ribosome contains two hybrid tRNAs (ASL of peptidyl-tRNA in the A-site, and ASL of deacyl-tRNA in the P-site). Finally, the tRNAs need to be translocated with their respective mRNA codons to the P and E ribosomal sites. Over the past two decades, a great deal of scientific effort has been invested in mechanistically describing translation elongation and how the accuracy of elongation is maintained. Here, we focus on recent time-resolved cryo-EM studies, which unveiled unknown details of the structural relationship between GTP hydrolysis, translation elongation factor rearrangements, and ribosome dynamics in native biochemical reactions (Carbone et al., 2021; Loveland et al., 2020).

3.1 | Decoding and proofreading

Ribosomes accurately decode mRNA by proofreading each aa-tRNA that is delivered to the ribosomal A-site by the elongation factor EF-Tu, a universally conserved GTPase, in a so-called ternary complex (Burnett et al., 2013; Hopfield, 1974). The high accuracy of the decoding process is remarkable, with only 10^{-3} to 10^{-5} errors per codon, which is important for the sustainability of life (Wohlgemuth et al., 2010; Zhang et al., 2015). The selection of appropriate (cognate) aa-tRNA involves two steps: initial decoding and proofreading.

Previously, some key intermediates of the decoding and proofreading process have been identified and visualized by extensive biochemical (Ieong et al., 2016; Kothe & Rodnina, 2006; Zhang et al., 2015), biophysical (Blanchard et al., 2004; Gonzalez et al., 2007; Liu et al., 2015), computational (Noel & Whitford, 2016; Warias et al., 2020), crystallographic (Demeshkina et al., 2012; Ogle et al., 2001; Schmeing et al., 2009), and single-particle cryo-EM studies (Fislage et al., 2018; Loveland et al., 2017). In general, the base-pairing between the aa-tRNA anticodon and mRNA codon in the decoding center (DC) of the 30S subunit results in EF-Tu catalyzed GTP hydrolysis, followed by rearrangement of the EF-Tu into a GDP-bound form, releasing the aa-tRNA and accommodating it into the A-site of the 50S subunit. All these studies confirmed that the structural dynamics of the 30S subunit is the driving force behind the decoding process.

A recent time-resolved cryo-EM study (Loveland et al., 2020) carried out an authentic biochemical reaction with cognate aa-tRNAs, EF-Tu, and GTP, revealing details of the structural rearrangements during decoding and proofreading events over the time scale of the GTP hydrolysis (Figure 3a). Initially, the ternary complex is delivered to the 30S subunit shoulder of the ribosome, and the ribosome with a vacant A-site selects a cognate aa-tRNA. The initial position of the ternary complex on the ribosome prevents codon-anticodon base pairing, as the anticodon of the aa-tRNA is 15 Å away from the A-site, and the 30S subunit is in the open conformation. In addition, the GTPase domain of EF-Tu is 10 Å away from the sarcin-ricin loop (SRL) of the 50S subunit, thus GTP-hydrolysis is prevented at this stage (Figure 3a,b).

Furthermore, the kinked and twisted conformations of ASL bring the cognate aa-tRNA close to the A-site and result in codon-anticodon base-pairing. The decoding nucleotides G530, A1492, and A1493 of the 16S rRNA assist in the stabilization of the hydrogen bond formation between the codon and anticodon, thus locking the Watson–Crick helix in the DC of the 30S subunit. At this point, the 30S subunit is in the closed conformation and the GTPase domain of the EF-Tu comes in contact with the SRL, resulting in rapid GTP hydrolysis (Loveland et al., 2020; Rodnina et al., 2017; Voorhees et al., 2010). In contrast, during decoding and proofreading, the near-cognate aa-tRNA only samples the 30S subunit in the open conformation. Here, the mRNA and near-cognate aa-tRNA are destabilized in the DC, and the decoding nucleotides are disengaged from the codon–anticodon helix. As the 30S subunit fails to sample the closed conformation to lock the near-cognate aa-tRNA, the aa-tRNA dissociates and is rejected from the ribosome during initial selection (Loveland et al., 2020) or proofreading (Ieong et al., 2016).

The pre-GTP hydrolysis states visualized the EF-Tu in a compact conformation oriented closer to the SRL with the switch regions (GTPase domain) ordered, representing the initial selection stage (Figure 3a,b). In the post GTP-hydrolysis states, the EF-Tu takes on an extended conformation (EF-Tu dependent proofreading) similar to tRNA-unbound EF-Tu.GDP structures (Polekhina et al., 1996) (Figure 3a,c,d). EF-Tu destabilizes the closed 30S subunit conformation in the pre- and post-GTP hydrolysis stage. GTP hydrolysis and phosphate release initiate the destabilization of the GTPase domain of EF-Tu by enabling the movement of the switch regions (Figure 3b–d). The switch regions refold and become sterically incompatible with binding to aa-tRNA (Figure 3d). In this conformation, the GTPase domain of EF-Tu is released from SRL (~30 Å away from SRL), but EF-Tu remains ordered and is held in place (Figure 3d). The late EF-Tu dissociation state shows both domains of EF-Tu being released from the acceptor arm of the aa-tRNA, while domain 3 of EF-Tu continues to act as a bridge between the elbow of the aa-tRNA and the L11 stalk (Figure 3e).

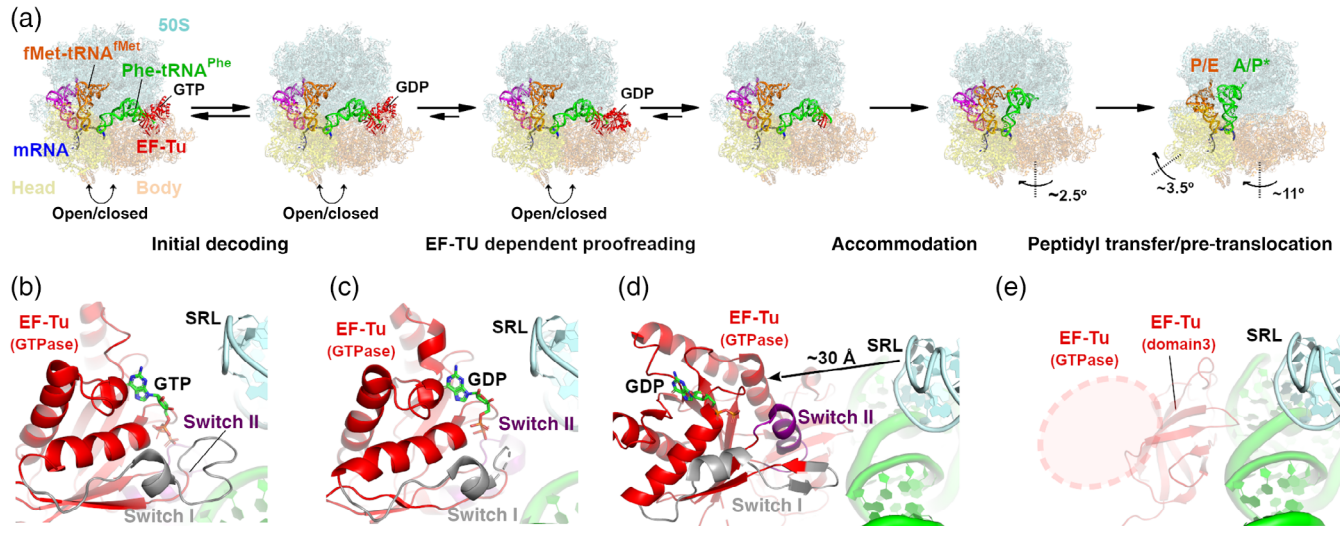

FIGURE 3 Structure-based view of mRNA decoding and tRNA proofreading. (a) Time-resolved cryo-EM trajectory showing initial decoding, EF-Tu dependent proofreading, tRNA accommodation (EF-Tu independent proofreading), peptidyl transfer, and pre-translocation. Close-up views of GTPase domain and switch regions of EF-Tu next to SRL in pre-GTP hydrolysis state (b), post-GTP hydrolysis states (c,d), and after partial EF-Tu dissociation (GTPase domain dissociation highlighted as transparent red circle) (e). The disordered switch regions are highlighted with a short dotted line. The double-ended curved arrows highlight the possible head tilt movement that generates open or closed conformations of the 30S subunit. The round arrows highlight the 30S body rotation or the 30S head swivel. The single arrow indicates the shift of the GTPase domain of EF-Tu after the switch regions refold.

After the release of EF-Tu, EF-Tu-independent proofreading starts. At this stage, the CCA end of the aa-tRNA is 80 Å away from the PTC of the 50S subunit. An ~2.5° rotation of the ribosome and movement of the A-site finger helps with the accommodation of the aa-tRNA into the A-site of the 50S subunit (Figure 3a). The structures of the accommodation states show that the 30S subunit remains in the closed state, with the cognate aa-tRNA stably locked in the DC of the 30S subunit. This indicates a commitment of the ribosome to accept the cognate tRNA. The insertion of the CCA moiety of the tRNA into the PTC of the 50S leads to peptidyl transfer. This results in the formation of the canonical deacyl-tRNA (P/E hybrid) in the P-site and a peptidyl-tRNA (A/P hybrid or elbow shifted A/P* hybrid) in the A-site with ~11° rotation of the 30S body and ~3.5° 30S head swivel (Figure 3a).

EF-Tu also has the ability of chiral proofreading, thus having a preference for L-amino acid carrying tRNAs (L-aa-tRNAs) over D-amino acid tRNAs (D-aa-tRNAs) (Ahmad et al., 2013; Kuncha et al., 2019). EF-Tu binding to L-aa-tRNAs is 25-fold stronger than for D-aa-tRNAs (Kuncha et al., 2019). This selection bias of EF-Tu toward the correct stereo-isomeric orientation of the respective amino acid (L-aa-tRNAs) is crucial for the ribosome to perform the protein synthesis. The D-aa-tRNAs can participate in the peptide synthesis (Englander et al., 2015), but with very poor efficiency (Fujino et al., 2013), as the rate of peptide bond formation is orders of magnitude slower (Yamane et al., 1981). A recent structural study of D-aa-tRNAs bound to the A-site of the ribosome (Melnikov et al., 2019) sheds more light on dipeptide formation when considering D-amino acids. Here, the non-optimal geometry of the D-amino acids causes a steric clash with the conserved U2506 nucleotide of the PTC. Due to the steric clash, the D-amino acids are kept at a distance from the A76 nucleotide of the P-site tRNA, which in turn may significantly slow down the peptide bond formation. However, to fully mechanistically understand the slow incorporation of D-amino acids during protein synthesis, ensemble or time-resolved cryo-EM studies could help to visualize the intermediate states of dipeptide formation.

3.2 | Translocation

In general, translocation is a series of steps encompassing the synchronous movement of mRNA and tRNAs through the ribosome (Ling & Ermolenko, 2016; Noller et al., 2017; Rodnina et al., 2019). Bacterial elongation factor G (EF-G), a conserved GTPase, catalyzes the translocation of the codon-anticodon base pairs of mRNA and the tRNAs in hybrid states to the P and E sites, respectively (Dorner et al., 2006; Holtkamp et al., 2014; Moazed & Noller, 1989b). Early biochemical (Moazed & Noller, 1989a, 1990), biophysical (Blanchard et al., 2004; Cornish et al., 2008; Munro et al., 2007) and structural studies (Agirrezabala et al., 2008; Cate et al., 1999; Frank & Agrawal, 2000; Horan & Noller, 2007; Julian et al., 2008) also indicated that large-scale ribosomal movement or intersubunit rotation, initially termed ratchet-like motion (Frank & Agrawal, 2000), is pivotal for translocation to occur.

The time scale (5–30 ms) of the GTP-accelerated EF-G dependent translocation (Rodnina et al., 1997; Wilden et al., 2006) posed a great challenge for structural studies to investigate the translocation event in real time. However, as suggested by kinetic studies (Katunin et al., 2002; Mohr et al., 2000; Rodnina et al., 1997), the rate of translocation decreased by 2- to 50-fold with EF-G in the presence of GDP, non-hydrolyzable GTP analogs or with GTPase-inactive mutants. Therefore, many structural studies tried to investigate the translocation by trapping EF-G with tRNAs on the ribosome in the presence of GTPase-inactive EF-G mutants (Li et al., 2015; Lin et al., 2015), antibiotics (Brilot et al., 2013; Gao et al., 2009; Lin et al., 2015; Petrychenko et al., 2021; Ramrath et al., 2013; Rundlet et al., 2021; Zhou et al., 2013), or non-hydrolyzable GTP analogs (Agrawal et al., 1999; Demo et al., 2021). However, these structural studies reported mainly strongly populated single-state structures due to the trapped EF-G on the ribosome. Some critical transient states of translocation were still elusive, leaving the structural picture of translocation unclear.

A recent time-resolved cryo-EM study (Carbone et al., 2021) captured translocation in a native GTP-catalyzed fast reaction, thus providing a detailed picture of pre-translocation substrates, EF-G-bound intermediates, and post-translocation products (Figure 4a). Initially, the peptidyl tRNA shifted ~25 Å toward the P-site, changing its state to an elbow-shifted A/P* state. This is accompanied by a reverse ~11° rotation of the 30S subunit, resulting in a pre-translocation state which acts as a substrate for EF-G to bind, consistent with biochemical observations (Ermolenko et al., 2007; Sharma et al., 2016). As the DC in the pre-translocation state is locked by decoding nucleotides G530, A1492, and A1493, EF-G has to unlock the DC for translocation to occur. The translocase domain 4 of EF-G is placed between dipeptidyl-tRNA and the DC of the 30S subunit. More specifically, loop 1 of translocase domain 4 comes in contact with G530, and loop 2 stabilizes the minor groove of helix 34 of 16S rRNA, keeping the 30S head in a pre-swiveled conformation, to unlock the DC. After binding to the ribosome, the EF-G adopts an extended conformation with the GTPase domain contacting the SRL and domain 5 binding the L11 stalk of the 50S subunit (Figure 4a,b).

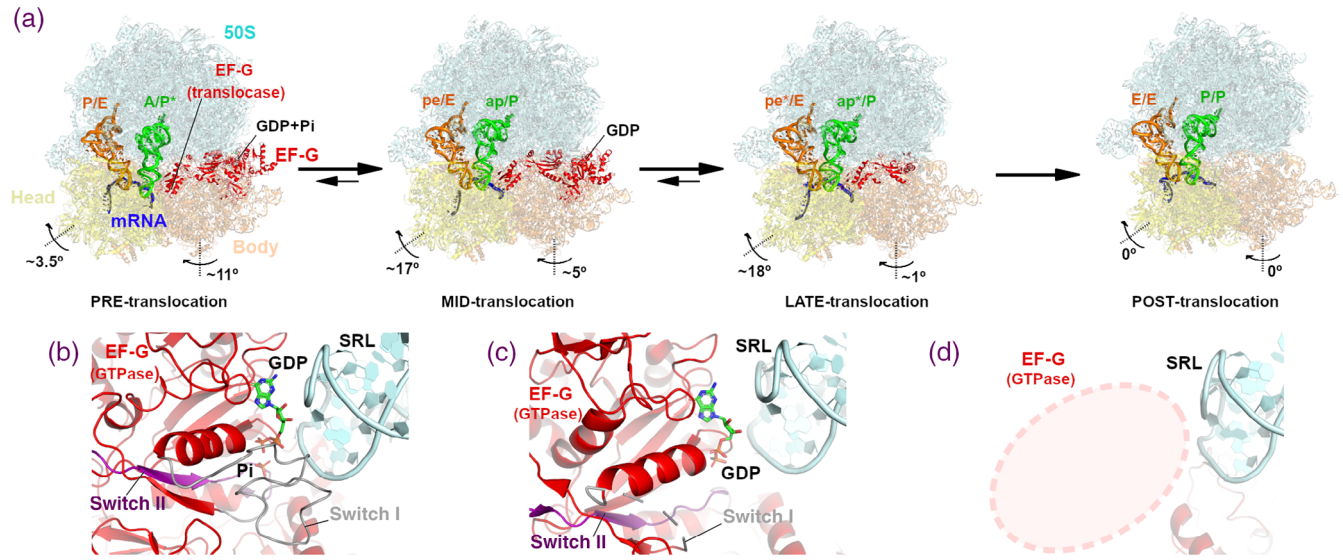

FIGURE 4 Time-ordered structural view of EF-G-catalyzed translocation. (a) Time-resolved cryo-EM trajectory showing the substrate, EF-G-bound intermediates, and the product. The tRNAs are highlighted in their respective states according to each translocation phase. Close-up views of the GTPase domain and switch regions of EF-G next to SRL in the GDP.Pi state (b), GDP state (c), and after partial EF-G dissociation (GTPase domain dissociation highlighted as transparent red circle) (d). The disordered switch regions are highlighted with a short dotted line. The curved arrows highlight the 30S body rotation or 30S head swivel.

The GTPase domain is in its activated conformation with GDP and Pi present in the active site, which are stabilized by ordered switch loops 1 and 2 (Figure 4b). In this post-GTP-hydrolysis state, the rotated 30S subunit prevents the release of Pi and early dissociation of EF-G before translocation.

During mid-translocation, a 5° reverse 30S subunit rotation occurs, whereas EF-G retains an extended conformation (Figure 4a). Translocase domain 4 shifts ~20 Å from its original position in the pre-translocation state, and is inserted into the A-site. For accommodation into the A-site, EF-G undergoes interdomain rearrangements similar to local fluctuations seen in unbound EF-G (Czworkowski et al., 1994; Salsi et al., 2015). Loops 1 and 2 of domain 4 move closer to the dipeptidyl-tRNA and mRNA, resulting in contact with the codon-anticodon helix. The separation of the dipeptidyl-tRNA from the DC is accompanied by an ~20 Å movement of the tRNA into the P-site and deacyl-tRNA into the E-site. This results in the chimeric ap/P and pe/E states of the tRNAs (Figure 4a), similar to the states visualized in the presence of fusidic acid (Ramrath et al., 2013). In combination with the EF-G movement, an ~17° 30S head rotation toward the tRNAs occurs, which extends contact with both tRNAs and the mRNA to maintain the ORF. The movement of EF-G into the A-site also separates the GTPase domain from the SRL (Figure 4c). The switch loops are destabilized (Figure 4c) due to the loss of contact between the reversely rotated 30S subunit and the GTPase domain. Pi is released with only GDP present in the GTPase center.

In the late-translocation state, an ~1° rotation of the body and an ~18° head swivel of the 30S subunit occur (Figure 4a), consistent with FRET studies (Guo & Noller, 2012; Wasserman et al., 2016). The tRNAs and translocase domain 4 of EF-G move 3–5 Å across the 30S, and the dipeptidyl-tRNA is found in an intermediate state to be fully translocated—the ap*/P conformation. Translocase domain 4 remains attached to the ribosome, while the GTPase domain is released from the ribosome (Figure 4d).

The cryo-EM structures explained the long-debated role of GTP in EF-G.GTP-catalyzed translocation. First, GTP enables the EF-G to bind to the pre-translocation conformation of the ribosome. Next, GTP is immediately hydrolyzed as the GTPase domain of EF-G creates an interaction with the SRL of the 50S subunit. The phosphate remains stabilized by the switch loop region in the binding pocket of the GTPase center thanks to the rotated 30S subunit. The reverse rotation of the 30S subunit results in destabilization of the switch loop region and phosphate release. The phosphate release and EF-G movement initiate the dissociation of the GTPase domain of EF-G to generate a non-rotated ribosome with a vacant A-site. Thus the GTP hydrolysis contributes to the completion of translocation that enables the dissociation of EF-G from the ribosome, whereas the EF-G transforms spontaneous ribosomal dynamics into translocation.

4 | TERMINATION

In bacteria, the termination process is mediated by class-1 release factors (RFs). These factors contain two domains, (i) the stop codon recognition domain and (ii) the catalytic domain responsible for the hydrolysis of the peptidyl-tRNA in the PTC (Korostelev, 2011). The two RFs, RF1 and RF2, recognize the universal stop codons, UAA/UAG and UAA/UGA, respectively, at the A-site of the 30S subunit (Korostelev et al., 2010; Laurberg et al., 2008; Weixlbaumer et al., 2008). The catalytic domain of RFs has a universally conserved GGQ motif, whereas the amide of glutamine is responsible for the nucleophilic attack on the peptidyl-tRNA that results in the hydrolysis of the ester linkage between the tRNA and the nascent polypeptide. A switch loop that links the catalytic and codon-recognition domains plays a pivotal role in termination accuracy. Overall, the termination process can be divided into three steps: RF-mediated recognition of the stop codon, hydrolysis of the ester bond of the peptidyl-tRNA, and dissociation of RFs to initiate ribosome dissociation for recycling (Rodnina, 2018). The dissociation of RF1 is mediated by the peptide release and a GTPase RF3, while RF2 can dissociate spontaneously (Adio et al., 2018; Gao et al., 2007).

Translation termination in bacteria does not involve proofreading, but the error rates of peptide release are extremely low and comparable to those for sense-codon decoding (Freistroffer et al., 2000). Therefore, it is thought that the hydrolysis of the peptidyl-tRNA and stop codon recognition must be strictly linked and coordinated (Korostelev, 2011). This coordination likely prevents the docking of the catalytic domain into the PTC before the recognition of a stop codon (compact/closed conformation). Upon stop codon recognition, a conformational change induces the docking of the GGQ motif into the PTC (extended/open conformation). Initially, this idea was supported by structural studies of free RFs predominantly found in a compact conformation (Shin et al., 2004; Vestergaard et al., 2001) as opposed to structural studies of ribosome-bound RFs being always found in an extended conformation (Korostelev et al., 2008; Laurberg et al., 2008; Weixlbaumer et al., 2008). Later, biochemical studies revealed the dynamic behavior of RFs (He & Green, 2010; Trappl & Joseph, 2016), indicating that the pre-termination ribosome initially interacts with a compact form of RFs and induces a large-scale rearrangement to enable the hydrolysis of the peptidyl-tRNA (Trappl & Joseph, 2016). More recent structural studies on the hyper-accurate mutant of RF1 with the antibiotic blasticidin (Svidritskiy & Korostelev, 2018) and on a bacterial rescue system containing stalled ribosomes with truncated mRNAs (without a stop codon), alternative rescue factor A (ArfA) and RF2 (Demo, Svidritskiy, et al., 2017; James et al., 2016) identified the presence of compact and extended conformations of RFs within the ribosome. However, capturing a canonical termination complex with RFs in both conformations remained challenging due to their rapid dynamic behavior (Hetrick et al., 2009; Trappl & Joseph, 2016).

A recent time-resolved cryo-EM study (Fu et al., 2019), using a mixing-spraying approach (Chen et al., 2015; Fu et al., 2016), captured intermediate states of the termination process in which both RF1 and RF2 were shown in both compact and extended states coupled with stop codon recognition and the hydrolysis of peptidyl-tRNA in the PTC (Figure 5). Initially, the RFs bind to the termination complex (non-rotated ribosome with stop codon in the A-site) in a compact state and recognize the stop codon in the DC of the 30S subunit, while the GGQ motif of RFs is ~60 Å away from the PTC (Figure 5a–c,e). The loop that contains the GGQ motif is positioned toward the anticodon-stem loop of the peptidyl-tRNA, forming a pre-accommodated-RF ribosome complex (Figure 5a,b). The subsequent intermediate state is the accommodated-RF ribosome complex, in which the RFs settle ~3 Å deeper into the DC, and the tip of the switch loop moves by ~20 Å to interact with A1492 in the DC. Due to switch loop stabilization, the RF switches from the compact to the extended conformation, positioning the GGQ motif within the PTC adjacent to the CCA end of the peptidyl-tRNA (Figure 5d,f). Moreover, a recent cryo-EM study (Svidritskiy et al., 2019) shows an additional conformational change in the catalytic domain of RF2. Here, as the CCA end of the peptidyl-tRNA is released from the PTC, the GGQ loop of RF2 rearranges from a short helix–loop into a β-hairpin structure that extends into the peptide exit tunnel. This rearrangement could allow the synthesized protein to dissociate from the ribosome.

The final state of termination is the released peptide RF-ribosome complex, in which the peptide has been released followed by dissociation of the deacylated tRNA from the ribosome, permitting 30S subunit rotation. The two cryo-EM studies elucidated the role of 30S subunit rotation and its implications on RF3-mediated RF1 dissociation (Graf et al., 2018) and RF2 dissociation without RF3 (Svidritskiy et al., 2019). In RF3-mediated RF1 dissociation, the binding of RF3 in the GTP conformation induces a partial 30S subunit rotation. The observed partial head swivel of the 30S subunit disrupts interactions with the codon-recognition domain and destabilizes RF1 or RF2 (Graf et al., 2018; Svidritskiy et al., 2019). The full rotation of the 30S subunit with hybrid P/E tRNA triggers the dissociation of RF1 (or RF2) and accommodation of the RF3 with the GTPase domain close to the SRL of the 50S subunit. This induces GTP hydrolysis and initiates the dissociation of the RF3.GDP state from the ribosome. Afterward, the fully rotated ribosome in post-

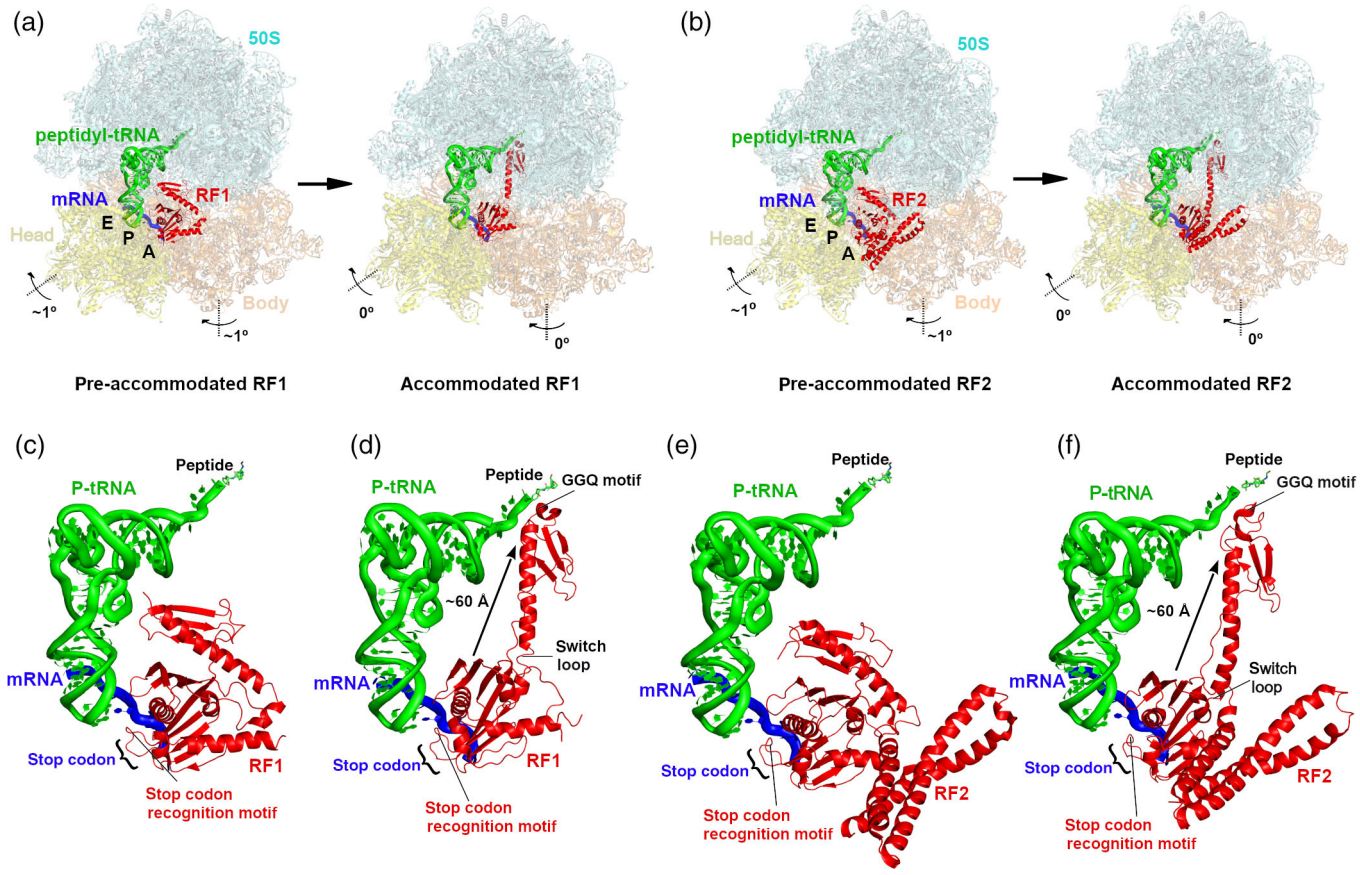

FIGURE 5 Structure-based view of RF1- and RF2-catalyzed termination. Time-resolved cryo-EM showing pre-accommodated and accommodated state for RF1 (a) and RF2 (b). The round arrows highlight the 30S body rotation or 30S head swivel. Close-up views of the pre-accommodated and accommodated state for RF1 and RF2 showing the stop codon recognition domain (c,e) and hydrolase domain in the activated state (d,f). The single arrow indicates the movement of the hydrolase domain of RF1 or RF2 after stop codon recognition.

termination (for both of the cases: RF1 or RF2) is recognized by the ribosome recycling factor (RRF) and EF-G to initiate ribosome recycling (subunit and tRNA dissociation) as elucidated by a time-resolved cryo-EM study (Fu et al., 2016).

5 | CONCLUSION

Over the past decade, time-resolved and ensemble cryo-EM have made significant progress in studying dynamic conformational changes of macromolecular complexes. In combination with other structural (e.g., protein crystallography) and biophysical methods (e.g., FRET), time-resolved and ensemble cryo-EM experiments have been accelerating the structural elucidation of vital biochemical processes at high resolution, giving a great example of an integrative structural biology approach. In bacteria, cryo-EM has helped to uncover various intermediate states of initiation, elongation, and termination (Carbone et al., 2021; Fu et al., 2019; Kaledhonkar et al., 2019; Loveland et al., 2020), which were previously unknown or only detected by single-molecule FRET studies. Future time-resolved cryo-EM studies are expected to play a key role in elucidating the initiation pathway in more detail, specifically the interplay between all three initiation factors, their organization, and conformational dynamics in the 30S IC and 70S IC complexes. Considering the time scale of EF-G dependent translocation (Rodnina et al., 1997), technological advancements in time-resolved cryo-EM (Dandey et al., 2020) should enable the visualization of additional intermediate states that elucidate the remaining gaps in the translocation mechanism. In addition, time-resolved cryo-EM studies can decipher some less well-understood processes of translation such as ribosome recycling, which could help to extend our understanding of the recycling mechanism from previous studies (Agrawal et al., 2004; Borg et al., 2016; Chen et al., 2017; Fu et al., 2016).

Although translation in bacteria is well understood at the molecular level, in recent years multiple cryo-EM studies concentrated to structurally describe translation events in eukaryotes, considering cytoplasmic (Brito Querido et al., 2020; Ranjan et al., 2021; Yi et al., 2022) or mitochondrial translation (Aibara et al., 2020; Koripella et al., 2020; Kummer & Ban, 2020). Here, by capturing intermediate states, time-resolved, and ensemble cryo-EM can offer a deep visualization of all phases of eukaryotic translation, which is more complex than in bacteria.

Moreover, there has been a recent rise in interest in obtaining detailed insights into the process of transcription and translation coupling in bacteria (Demo, Rasouly, et al., 2017; Kohler et al., 2017; O'Reilly et al., 2020; Wang et al., 2020; Webster et al., 2020). As the bacteria lack a physical barrier (i.e., a nuclear membrane), transcription and translation machineries can be coupled, thus enabling the newly transcribed mRNAs to be immediately bound by ribosomes (Conn et al., 2019; Irastortza-Olaziregi & Amster-Choder, 2020). The transcription–translation coupling complexes in these studies show dynamic ribosome interactions with RNA polymerase in the presence of transcription factors. To discover the mechanistic details of coupled systems, future time-resolved cryo-EM studies should be able to determine the intermediate states of the complexes and reveal the ribosome and RNA polymerase motions in an active coupled system involving the transcription and translation factors.

Time-resolved and ensemble cryo-EM comes with shortcomings such as optimizing fast reactions on the grid, and time-consuming as well as computationally demanding data analysis. However, visualizing biological processes and their intermediate states via cryo-EM at different time scales could be preferred by biologists. The future seems to hold exciting times, especially for time-resolved cryo-EM studies, whereas further improvements in methodologies could help to understand native cellular processes at the atomic level.

AUTHOR CONTRIBUTIONS

Hassan Zafar: Methodology (equal); validation (equal); visualization (lead); writing – original draft (equal); writing – review and editing (supporting). **Ahmed Hassan:** Validation (supporting); visualization (supporting). **Gabriel Demo:** Conceptualization (lead); funding acquisition (lead); investigation (lead); methodology (equal); validation (equal); writing – original draft (equal); writing – review and editing (lead).

FUNDING INFORMATION

We would like to thank the members of the Demo lab for their comments on the manuscript. This work was supported by the LL2008 project with financial support from the MEYS CR as a part of the ERC CZ program and the project National Institute of virology and bacteriology (Programme EXCELES, ID Project No. LX22NPO5103)—Funded by the European Union—Next Generation EU.

CONFLICT OF INTEREST STATEMENT

The authors have declared no conflicts of interest for this article.

DATA AVAILABILITY STATEMENT

Data sharing is not applicable to this article as no new data were created or analyzed in this study.

ORCID

Hassan Zafar https://orcid.org/0000-0001-7600-0734
Gabriel Demo https://orcid.org/0000-0002-5472-9249

RELATED WIREs ARTICLES

Structural insights into ribosome translocation

REFERENCES

Adio, S., Sharma, H., Senyushkina, T., Karki, P., Maracci, C., Wohlgemuth, I., Holtkamp, W., Peske, F., & Rodnina, M. V. (2018). Dynamics of ribosomes and release factors during translation termination in *E. coli*. *eLife*, *7*, e34252. https://doi.org/10.7554/eLife.34252

Agirrezabala, X., Lei, J., Brunelle, J. L., Ortiz-Meoz, R. F., Green, R., & Frank, J. (2008). Visualization of the hybrid state of tRNA binding promoted by spontaneous ratcheting of the ribosome. *Molecular Cell*, *32*(2), 190–197. https://doi.org/10.1016/j.molcel.2008.10.001

Agrawal, R. K., Heagle, A. B., Penczek, P., Grassucci, R. A., & Frank, J. (1999). EF-G-dependent GTP hydrolysis induces translocation accompanied by large conformational changes in the 70S ribosome. *Nature Structural Biology*, *6*(7), 643–647. https://doi.org/10.1038/10695

Agrawal, R. K., Sharma, M. R., Kiel, M. C., Hirokawa, G., Booth, T. M., Spahn, C. M., Grassucci, R. A., Kaji, A., & Frank, J. (2004). Visualization of ribosome-recycling factor on the *Escherichia coli* 70S ribosome: functional implications. *Proceedings of the National Academy of Sciences of the United States of America*, *101*(24), 8900–8905. https://doi.org/10.1073/pnas.0401904101

Ahmad, S., Routh, S. B., Kamarthapu, V., Chalissery, J., Muthukumar, S., Hussain, T., Kruparani, S. P., Deshmukh, M. V., & Sankaranarayanan, R. (2013). Mechanism of chiral proofreading during translation of the genetic code. *eLife*, *2*, e01519. https://doi.org/10.7554/eLife.01519

Aibara, S., Singh, V., Modelska, A., & Amunts, A. (2020). Structural basis of mitochondrial translation. *eLife*, *9*, e58362. https://doi.org/10.7554/eLife.58362

Allen, G. S., Zavialov, A., Gursky, R., Ehrenberg, M., & Frank, J. (2005). The cryo-EM structure of a translation initiation complex from *Escherichia coli*. *Cell*, *121*(5), 703–712. https://doi.org/10.1016/j.cell.2005.03.023

Antoun, A., Pavlov, M. Y., Andersson, K., Tenson, T., & Ehrenberg, M. (2003). The roles of initiation factor 2 and guanosine triphosphate in initiation of protein synthesis. *The EMBO Journal*, *22*(20), 5593–5601. https://doi.org/10.1093/emboj/cdg525

Antoun, A., Pavlov, M. Y., Lovmar, M., & Ehrenberg, M. (2006a). How initiation factors maximize the accuracy of tRNA selection in initiation of bacterial protein synthesis. *Molecular Cell*, *23*(2), 183–193. https://doi.org/10.1016/j.molcel.2006.05.030

Antoun, A., Pavlov, M. Y., Lovmar, M., & Ehrenberg, M. (2006b). How initiation factors tune the rate of initiation of protein synthesis in bacteria. *The EMBO Journal*, *25*(11), 2539–2550. https://doi.org/10.1038/sj.emboj.7601140

Basu, R. S., Sherman, M. B., & Gagnon, M. G. (2022). Compact IF2 allows initiator tRNA accommodation into the P site and gates the ribosome to elongation. *Nature Communications*, *13*(1), 3388. https://doi.org/10.1038/s41467-022-31129-2

Belardinelli, R., Sharma, H., Caliskan, N., Cunha, C. E., Peske, F., Wintermeyer, W., & Rodnina, M. V. (2016). Choreography of molecular movements during ribosome progression along mRNA. *Nature Structural & Molecular Biology*, *23*(4), 342–348. https://doi.org/10.1038/nsmb.3193

Blanchard, S. C., Kim, H. D., Gonzalez, R. L., Jr., Puglisi, J. D., & Chu, S. (2004). tRNA dynamics on the ribosome during translation. *Proceedings of the National Academy of Sciences of the United States of America*, *101*(35), 12893–12898. https://doi.org/10.1073/pnas.0403884101

Borg, A., Pavlov, M., & Ehrenberg, M. (2016). Complete kinetic mechanism for recycling of the bacterial ribosome. *RNA*, *22*(1), 10–21. https://doi.org/10.1261/rna.053157.115

Brilot, A. F., Chen, J. Z., Cheng, A., Pan, J., Harrison, S. C., Potter, C. S., Carragher, B., Henderson, R., & Grigorieff, N. (2012). Beam-induced motion of vitrified specimen on holey carbon film. *Journal of Structural Biology*, *177*(3), 630–637. https://doi.org/10.1016/j.jsb.2012.02.003

Brilot, A. F., Korostelev, A. A., Ermolenko, D. N., & Grigorieff, N. (2013). Structure of the ribosome with elongation factor G trapped in the pretranslocation state. *Proceedings of the National Academy of Sciences of the United States of America*, *110*(52), 20994–20999. https://doi.org/10.1073/pnas.1311423110

Brito Querido, J., Sokabe, M., Kraatz, S., Gordiyenko, Y., Skehel, J. M., Fraser, C. S., & Ramakrishnan, V. (2020). Structure of a human 48S translational initiation complex. *Science*, *369*(6508), 1220–1227. https://doi.org/10.1126/science.aba4904

Burnett, B. J., Altman, R. B., Ferrao, R., Alejo, J. L., Kaur, N., Kanji, J., & Blanchard, S. C. (2013). Elongation factor Ts directly facilitates the formation and disassembly of the *Escherichia coli* elongation factor Tu.GTP.aminoacyl-tRNA ternary complex. *The Journal of Biological Chemistry*, *288*(19), 13917–13928. https://doi.org/10.1074/jbc.M113.460014

Byrgazov, K., Vesper, O., & Moll, I. (2013). Ribosome heterogeneity: another level of complexity in bacterial translation regulation. *Current Opinion in Microbiology*, *16*(2), 133–139. https://doi.org/10.1016/j.mib.2013.01.009

Carbone, C. E., Loveland, A. B., Gamper, H. B., Jr., Hou, Y. M., Demo, G., & Korostelev, A. A. (2021). Time-resolved cryo-EM visualizes ribosomal translocation with EF-G and GTP. *Nature Communications*, *12*(1), 7236. https://doi.org/10.1038/s41467-021-27415-0

Cate, J. H., Yusupov, M. M., Yusupova, G. Z., Earnest, T. N., & Noller, H. F. (1999). X-ray crystal structures of 70S ribosome functional complexes. *Science*, *285*(5436), 2095–2104. https://doi.org/10.1126/science.285.5436.2095

Chen, B., Kaledhonkar, S., Sun, M., Shen, B., Lu, Z., Barnard, D., Lu, T. M., Gonzalez, R. L., Jr., & Frank, J. (2015). Structural dynamics of ribosome subunit association studied by mixing-spraying time-resolved cryogenic electron microscopy. *Structure*, *23*(6), 1097–1105. https://doi.org/10.1016/j.str.2015.04.007

Chen, Y., Kaji, A., Kaji, H., & Cooperman, B. S. (2017). The kinetic mechanism of bacterial ribosome recycling. *Nucleic Acids Research*, *45*(17), 10168–10177. https://doi.org/10.1093/nar/gkx694

Conn, A. B., Diggs, S., Tam, T. K., & Blaha, G. M. (2019). Two old dogs, one new trick: A review of RNA polymerase and ribosome interactions during transcription-translation coupling. *International Journal of Molecular Sciences*, *20*(10), 2595. https://doi.org/10.3390/ijms20102595

Cornish, P. V., Ermolenko, D. N., Noller, H. F., & Ha, T. (2008). Spontaneous intersubunit rotation in single ribosomes. *Molecular Cell*, *30*(5), 578–588. https://doi.org/10.1016/j.molcel.2008.05.004

Czworkowski, J., Wang, J., Steitz, T. A., & Moore, P. B. (1994). The crystal structure of elongation factor G complexed with GDP, at 2.7 A resolution. *The EMBO Journal*, *13*(16), 3661–3668. https://doi.org/10.1002/j.1460-2075.1994.tb06675.x

Dandey, V. P., Budell, W. C., Wei, H., Bobe, D., Maruthi, K., Kopylov, M., Eng, E. T., Kahn, P. A., Hinshaw, J. E., Kundu, N., Nimigean, C. M., Fan, C., Sukomon, N., Darst, S. A., Saecker, R. M., Chen, J., Malone, B., Potter, C. S., & Carragher, B. (2020). Time-resolved cryo-EM using Spotiton. *Nature Methods*, *17*(9), 897–900. https://doi.org/10.1038/s41592-020-0925-6

Demeshkina, N., Jenner, L., Westhof, E., Yusupov, M., & Yusupova, G. (2012). A new understanding of the decoding principle on the ribosome. *Nature*, *484*(7393), 256–259. https://doi.org/10.1038/nature10913

Demo, G., Gamper, H. B., Loveland, A. B., Masuda, I., Carbone, C. E., Svidritskiy, E., Hou, Y. M., & Korostelev, A. A. (2021). Structural basis for +1 ribosomal frameshifting during EF-G-catalyzed translocation. *Nature Communications*, *12*(1), 4644. https://doi.org/10.1038/s41467-021-24911-1

Demo, G., Rasouly, A., Vasilyev, N., Svetlov, V., Loveland, A. B., Diaz-Avalos, R., Grigorieff, N., Nudler, E., & Korostelev, A. A. (2017). Structure of RNA polymerase bound to ribosomal 30S subunit. *eLife*, *6*, e28560. https://doi.org/10.7554/eLife.28560

Demo, G., Svidritskiy, E., Madireddy, R., Diaz-Avalos, R., Grant, T., Grigorieff, N., Sousa, D., & Korostelev, A. A. (2017). Mechanism of ribosome rescue by ArfA and RF2. *eLife*, *6*, e23687. https://doi.org/10.7554/eLife.23687

Dorner, S., Brunelle, J. L., Sharma, D., & Green, R. (2006). The hybrid state of tRNA binding is an authentic translation elongation intermediate. *Nature Structural & Molecular Biology*, *13*(3), 234–241. https://doi.org/10.1038/nsmb1060

Earl, L. A., Falconieri, V., Milne, J. L., & Subramaniam, S. (2017). Cryo-EM: beyond the microscope. *Current Opinion in Structural Biology*, *46*, 71–78. https://doi.org/10.1016/j.sbi.2017.06.002

Elvekrog, M. M., & Gonzalez, R. L., Jr. (2013). Conformational selection of translation initiation factor 3 signals proper substrate selection. *Nature Structural & Molecular Biology*, *20*(5), 628–633. https://doi.org/10.1038/nsmb.2554

Englander, M. T., Avins, J. L., Fleisher, R. C., Liu, B., Effraim, P. R., Wang, J., Schulten, K., Leyh, T. S., Gonzalez, R. L., Jr., & Cornish, V. W. (2015). The ribosome can discriminate the chirality of amino acids within its peptidyl-transferase center. *Proceedings of the National Academy of Sciences of the United States of America*, *112*(19), 6038–6043. https://doi.org/10.1073/pnas.1424712112

Ermolenko, D. N., Majumdar, Z. K., Hickerson, R. P., Spiegel, P. C., Clegg, R. M., & Noller, H. F. (2007). Observation of intersubunit movement of the ribosome in solution using FRET. *Journal of Molecular Biology*, *370*(3), 530–540. https://doi.org/10.1016/j.jmb.2007.04.042

Fischer, N., Neumann, P., Konevega, A. L., Bock, L. V., Ficner, R., Rodnina, M. V., & Stark, H. (2015). Structure of the *E. coli* ribosome-EF-Tu complex at <3 A resolution by Cs-corrected cryo-EM. *Nature*, *520*(7548), 567–570. https://doi.org/10.1038/nature14275

Fislage, M., Zhang, J., Brown, Z. P., Mandava, C. S., Sanyal, S., Ehrenberg, M., & Frank, J. (2018). Cryo-EM shows stages of initial codon selection on the ribosome by aa-tRNA in ternary complex with GTP and the GTPase-deficient EF-TuH84A. *Nucleic Acids Research*, *46*(11), 5861–5874. https://doi.org/10.1093/nar/gky346

Frank, J. (2017). Time-resolved cryo-electron microscopy: Recent progress. *Journal of Structural Biology*, *200*(3), 303–306. https://doi.org/10.1016/j.jsb.2017.06.005

Frank, J., & Agrawal, R. K. (2000). A ratchet-like inter-subunit reorganization of the ribosome during translocation. *Nature*, *406*(6793), 318–322. https://doi.org/10.1038/35018597

Frank, J., Gao, H., Sengupta, J., Gao, N., & Taylor, D. J. (2007). The process of mRNA-tRNA translocation. *Proceedings of the National Academy of Sciences of the United States of America*, *104*(50), 19671–19678. https://doi.org/10.1073/pnas.0708517104

Frank, J., & Gonzalez, R. L., Jr. (2010). Structure and dynamics of a processive Brownian motor: the translating ribosome. *Annual Review of Biochemistry*, *79*, 381–412. https://doi.org/10.1146/annurev-biochem-060408-173330

Freistroffer, D. V., Kwiatkowski, M., Buckingham, R. H., & Ehrenberg, M. (2000). The accuracy of codon recognition by polypeptide release factors. *Proceedings of the National Academy of Sciences of the United States of America*, *97*(5), 2046–2051. https://doi.org/10.1073/pnas.030541097

Fu, Z., Indrisiunaite, G., Kaledhonkar, S., Shah, B., Sun, M., Chen, B., Grassucci, R. A., Ehrenberg, M., & Frank, J. (2019). The structural basis for release-factor activation during translation termination revealed by time-resolved cryogenic electron microscopy. *Nature Communications*, *10*(1), 2579. https://doi.org/10.1038/s41467-019-10608-z

Fu, Z., Kaledhonkar, S., Borg, A., Sun, M., Chen, B., Grassucci, R. A., Ehrenberg, M., & Frank, J. (2016). Key intermediates in ribosome recycling visualized by time-resolved cryoelectron microscopy. *Structure*, *24*(12), 2092–2101. https://doi.org/10.1016/j.str.2016.09.014

Fujino, T., Goto, Y., Suga, H., & Murakami, H. (2013). Reevaluation of the D-amino acid compatibility with the elongation event in translation. *Journal of the American Chemical Society*, *135*(5), 1830–1837. https://doi.org/10.1021/ja309570x

Gao, H., Zhou, Z., Rawat, U., Huang, C., Bouakaz, L., Wang, C., Cheng, Z., Liu, Y., Zavialov, A., Gursky, R., Sanyal, S., Ehrenberg, M., Frank, J., & Song, H. (2007). RF3 induces ribosomal conformational changes responsible for dissociation of class I release factors. *Cell*, *129*(5), 929–941. https://doi.org/10.1016/j.cell.2007.03.050

Gao, Y. G., Selmer, M., Dunham, C. M., Weixlbaumer, A., Kelley, A. C., & Ramakrishnan, V. (2009). The structure of the ribosome with elongation factor G trapped in the posttranslocational state. *Science*, *326*(5953), 694–699. https://doi.org/10.1126/science.1179709

Gonzalez, R. L., Jr., Chu, S., & Puglisi, J. D. (2007). Thiostrepton inhibition of tRNA delivery to the ribosome. *RNA*, *13*(12), 2091–2097. https://doi.org/10.1261/rna.499407

Goyal, A., Belardinelli, R., Maracci, C., Milon, P., & Rodnina, M. V. (2015). Directional transition from initiation to elongation in bacterial translation. *Nucleic Acids Research*, *43*(22), 10700–10712. https://doi.org/10.1093/nar/gkv869

Graf, M., Huter, P., Maracci, C., Peterek, M., Rodnina, M. V., & Wilson, D. N. (2018). Visualization of translation termination intermediates trapped by the Apidaecin 137 peptide during RF3-mediated recycling of RF1. *Nature Communications*, *9*(1), 3053. https://doi.org/10.1038/s41467-018-05465-1

Grigoriadou, C., Marzi, S., Kirillov, S., Gualerzi, C. O., & Cooperman, B. S. (2007). A quantitative kinetic scheme for 70 S translation initiation complex formation. *Journal of Molecular Biology*, *373*(3), 562–572. https://doi.org/10.1016/j.jmb.2007.07.032

Grigoriadou, C., Marzi, S., Pan, D., Gualerzi, C. O., & Cooperman, B. S. (2007). The translational fidelity function of IF3 during transition from the 30 S initiation complex to the 70 S initiation complex. *Journal of Molecular Biology*, *373*(3), 551–561. https://doi.org/10.1016/j.jmb.2007.07.031

Grigorieff, N. (2016). Frealign: An exploratory tool for single-particle cryo-EM. *Methods in Enzymology*, *579*, 191–226. https://doi.org/10.1016/bs.mie.2016.04.013

Guo, Z., & Noller, H. F. (2012). Rotation of the head of the 30S ribosomal subunit during mRNA translocation. *Proceedings of the National Academy of Sciences of the United States of America*, *109*(50), 20391–20394. https://doi.org/10.1073/pnas.1218999109

He, S. L., & Green, R. (2010). Visualization of codon-dependent conformational rearrangements during translation termination. *Nature Structural & Molecular Biology*, *17*(4), 465–470. https://doi.org/10.1038/nsmb.1766

Hershey, J. W., Sonenberg, N., & Mathews, M. B. (2012). Principles of translational control: an overview. *Cold Spring Harbor Perspectives in Biology*, *4*(12), a011528. https://doi.org/10.1101/cshperspect.a011528

Hetrick, B., Lee, K., & Joseph, S. (2009). Kinetics of stop codon recognition by release factor 1. *Biochemistry*, *48*(47), 11178–11184. https://doi.org/10.1021/bi901577d

Holtkamp, W., Cunha, C. E., Peske, F., Konevega, A. L., Wintermeyer, W., & Rodnina, M. V. (2014). GTP hydrolysis by EF-G synchronizes tRNA movement on small and large ribosomal subunits. *The EMBO Journal*, *33*(9), 1073–1085. https://doi.org/10.1002/embj.201387465

Hopfield, J. J. (1974). Kinetic proofreading: a new mechanism for reducing errors in biosynthetic processes requiring high specificity. *Proceedings of the National Academy of Sciences of the United States of America*, *71*(10), 4135–4139. https://doi.org/10.1073/pnas.71.10.4135

Horan, L. H., & Noller, H. F. (2007). Intersubunit movement is required for ribosomal translocation. *Proceedings of the National Academy of Sciences of the United States of America*, *104*(12), 4881–4885. https://doi.org/10.1073/pnas.0700762104

Hussain, T., Llacer, J. L., Wimberly, B. T., Kieft, J. S., & Ramakrishnan, V. (2016). Large-scale movements of IF3 and tRNA during bacterial translation initiation. *Cell*, *167*(1), 133–144. https://doi.org/10.1016/j.cell.2016.08.074

Ieong, K. W., Uzun, U., Selmer, M., & Ehrenberg, M. (2016). Two proofreading steps amplify the accuracy of genetic code translation. *Proceedings of the National Academy of Sciences of the United States of America*, *113*(48), 13744–13749. https://doi.org/10.1073/pnas.1610917113

Indrisiunaite, G., Pavlov, M. Y., Heurgue-Hamard, V., & Ehrenberg, M. (2015). On the pH dependence of class-1 RF-dependent termination of mRNA translation. *Journal of Molecular Biology*, *427*(9), 1848–1860. https://doi.org/10.1016/j.jmb.2015.01.007

Irastortza-Olaziregi, M., & Amster-Choder, O. (2020). Coupled transcription-translation in prokaryotes: An old couple with new surprises. *Frontiers in Microbiology*, *11*, 624830. https://doi.org/10.3389/fmicb.2020.624830

James, N. R., Brown, A., Gordiyenko, Y., & Ramakrishnan, V. (2016). Translational termination without a stop codon. *Science*, *354*(6318), 1437–1440. https://doi.org/10.1126/science.aai9127

Julian, P., Konevega, A. L., Scheres, S. H., Lazaro, M., Gil, D., Wintermeyer, W., Rodnina, M. V., & Valle, M. (2008). Structure of ratcheted ribosomes with tRNAs in hybrid states. *Proceedings of the National Academy of Sciences of the United States of America*, *105*(44), 16924–16927. https://doi.org/10.1073/pnas.0809587105

Julian, P., Milon, P., Agirrezabala, X., Lasso, G., Gil, D., Rodnina, M. V., & Valle, M. (2011). The Cryo-EM structure of a complete 30S translation initiation complex from *Escherichia coli*. *PLoS Biology*, *9*(7), e1001095. https://doi.org/10.1371/journal.pbio.1001095

Kaczanowska, M., & Ryden-Aulin, M. (2007). Ribosome biogenesis and the translation process in *Escherichia coli*. *Microbiology and Molecular Biology Reviews*, *71*(3), 477–494. https://doi.org/10.1128/MMBR.00013-07

Kaledhonkar, S., Fu, Z., Caban, K., Li, W., Chen, B., Sun, M., Gonzalez, R. L., Jr., & Frank, J. (2019). Late steps in bacterial translation initiation visualized using time-resolved cryo-EM. *Nature*, *570*(7761), 400–404. https://doi.org/10.1038/s41586-019-1249-5

Katunin, V. I., Savelsbergh, A., Rodnina, M. V., & Wintermeyer, W. (2002). Coupling of GTP hydrolysis by elongation factor G to translocation and factor recycling on the ribosome. *Biochemistry*, *41*(42), 12806–12812. https://doi.org/10.1021/bi0264871

Kohler, R., Mooney, R. A., Mills, D. J., Landick, R., & Cramer, P. (2017). Architecture of a transcribing-translating expressome. *Science*, *356*(6334), 194–197. https://doi.org/10.1126/science.aal3059

Koripella, R. K., Sharma, M. R., Bhargava, K., Datta, P. P., Kaushal, P. S., Keshavan, P., Spremulli, L. L., Banavali, N. K., & Agrawal, R. K. (2020). Structures of the human mitochondrial ribosome bound to EF-G1 reveal distinct features of mitochondrial translation elongation. *Nature Communications*, *11*(1), 3830. https://doi.org/10.1038/s41467-020-17715-2

Korostelev, A., Asahara, H., Lancaster, L., Laurberg, M., Hirschi, A., Zhu, J., Trakhanov, S., Scott, W. G., & Noller, H. F. (2008). Crystal structure of a translation termination complex formed with release factor RF2. *Proceedings of the National Academy of Sciences of the United States of America*, *105*(50), 19684–19689. https://doi.org/10.1073/pnas.0810953105

Korostelev, A., Zhu, J., Asahara, H., & Noller, H. F. (2010). Recognition of the amber UAG stop codon by release factor RF1. *The EMBO Journal*, *29*(15), 2577–2585. https://doi.org/10.1038/emboj.2010.139

Korostelev, A. A. (2011). Structural aspects of translation termination on the ribosome. *RNA*, *17*(8), 1409–1421. https://doi.org/10.1261/rna.2733411

Korostelev, A. A. (2022). The structural dynamics of translation. *Annual Review of Biochemistry*, *91*, 245–267. https://doi.org/10.1146/annurev-biochem-071921-122857

Kothe, U., & Rodnina, M. V. (2006). Delayed release of inorganic phosphate from elongation factor Tu following GTP hydrolysis on the ribosome. *Biochemistry*, *45*(42), 12767–12774. https://doi.org/10.1021/bi061192z

Kummer, E., & Ban, N. (2020). Structural insights into mammalian mitochondrial translation elongation catalyzed by mtEFG1. *The EMBO Journal*, *39*(15), e104820. https://doi.org/10.15252/embj.2020104820

Kuncha, S. K., Kruparani, S. P., & Sankaranarayanan, R. (2019). Chiral checkpoints during protein biosynthesis. *The Journal of Biological Chemistry*, *294*(45), 16535–16548. https://doi.org/10.1074/jbc.REV119.008166

Lancaster, M. E., Shelhamer, R., & Homa, D. (2013). Category inference as a function of correlational structure, category discriminability, and number of available cues. *Memory & Cognition*, *41*(3), 339–353. https://doi.org/10.3758/s13421-012-0271-8

Laurberg, M., Asahara, H., Korostelev, A., Zhu, J., Trakhanov, S., & Noller, H. F. (2008). Structural basis for translation termination on the 70S ribosome. *Nature*, *454*(7206), 852–857. https://doi.org/10.1038/nature07115

Laursen, B. S., Sorensen, H. P., Mortensen, K. K., & Sperling-Petersen, H. U. (2005). Initiation of protein synthesis in bacteria. *Microbiology and Molecular Biology Reviews*, *69*(1), 101–123. https://doi.org/10.1128/MMBR.69.1.101-123.2005

Li, W., Liu, Z., Koripella, R. K., Langlois, R., Sanyal, S., & Frank, J. (2015). Activation of GTP hydrolysis in mRNA-tRNA translocation by elongation factor G. *Science Advances*, *1*(4), e1500169. https://doi.org/10.1126/sciadv.1500169

Lin, J., Gagnon, M. G., Bulkley, D., & Steitz, T. A. (2015). Conformational changes of elongation factor G on the ribosome during tRNA translocation. *Cell*, *160*(1-2), 219–227. https://doi.org/10.1016/j.cell.2014.11.049

Ling, C., & Ermolenko, D. N. (2016). Structural insights into ribosome translocation. *Wiley Interdisciplinary Reviews: RNA*, *7*(5), 620–636. https://doi.org/10.1002/wrna.1354

Liu, W., Chen, C., Kavaliauskas, D., Knudsen, C. R., Goldman, Y. E., & Cooperman, B. S. (2015). EF-Tu dynamics during pre-translocation complex formation: EF-Tu.GDP exits the ribosome via two different pathways. *Nucleic Acids Research*, *43*(19), 9519–9528. https://doi.org/10.1093/nar/gkv856

Loveland, A. B., Demo, G., Grigorieff, N., & Korostelev, A. A. (2017). Ensemble cryo-EM elucidates the mechanism of translation fidelity. *Nature*, *546*(7656), 113–117. https://doi.org/10.1038/nature22397

Loveland, A. B., Demo, G., & Korostelev, A. A. (2020). Cryo-EM of elongating ribosome with EF-Tu*GTP elucidates tRNA proofreading. *Nature*, *584*(7822), 640–645. https://doi.org/10.1038/s41586-020-2447-x

Marshall, R. A., Aitken, C. E., & Puglisi, J. D. (2009). GTP hydrolysis by IF2 guides progression of the ribosome into elongation. *Molecular Cell*, *35*(1), 37–47. https://doi.org/10.1016/j.molcel.2009.06.008

McCutcheon, J. P., Agrawal, R. K., Philips, S. M., Grassucci, R. A., Gerchman, S. E., Clemons, W. M., Jr., Ramakrishnan, V., & Frank, J. (1999). Location of translational initiation factor IF3 on the small ribosomal subunit. *Proceedings of the National Academy of Sciences of the United States of America*, *96*(8), 4301–4306. https://doi.org/10.1073/pnas.96.8.4301

Melnikov, S. V., Khabibullina, N. F., Mairhofer, E., Vargas-Rodriguez, O., Reynolds, N. M., Micura, R., Soll, D., & Polikanov, Y. S. (2019). Mechanistic insights into the slow peptide bond formation with D-amino acids in the ribosomal active site. *Nucleic Acids Research*, *47*(4), 2089–2100. https://doi.org/10.1093/nar/gky1211

Milon, P., Konevega, A. L., Gualerzi, C. O., & Rodnina, M. V. (2008). Kinetic checkpoint at a late step in translation initiation. *Molecular Cell*, *30*(6), 712–720. https://doi.org/10.1016/j.molcel.2008.04.014

Milon, P., Maracci, C., Filonava, L., Gualerzi, C. O., & Rodnina, M. V. (2012). Real-time assembly landscape of bacterial 30S translation initiation complex. *Nature Structural & Molecular Biology*, *19*(6), 609–615. https://doi.org/10.1038/nsmb.2285

Moazed, D., & Noller, H. F. (1989a). Interaction of tRNA with 23S rRNA in the ribosomal A, P, and E sites. *Cell*, *57*(4), 585–597. https://doi.org/10.1016/0092-8674(89)90128-1

Moazed, D., & Noller, H. F. (1989b). Intermediate states in the movement of transfer RNA in the ribosome. *Nature*, *342*(6246), 142–148. https://doi.org/10.1038/342142a0

Moazed, D., & Noller, H. F. (1990). Binding of tRNA to the ribosomal A and P sites protects two distinct sets of nucleotides in 16 S rRNA. *Journal of Molecular Biology*, *211*(1), 135–145. https://doi.org/10.1016/0022-2836(90)90016-F

Mohr, D., Wintermeyer, W., & Rodnina, M. V. (2000). Arginines 29 and 59 of elongation factor G are important for GTP hydrolysis or translocation on the ribosome. *The EMBO Journal*, *19*(13), 3458–3464. https://doi.org/10.1093/emboj/19.13.3458

Munro, J. B., Altman, R. B., O'Connor, N., & Blanchard, S. C. (2007). Identification of two distinct hybrid state intermediates on the ribosome. *Molecular Cell*, *25*(4), 505–517. https://doi.org/10.1016/j.molcel.2007.01.022

Myasnikov, A. G., Marzi, S., Simonetti, A., Giuliodori, A. M., Gualerzi, C. O., Yusupova, G., Yusupov, M., & Klaholz, B. P. (2005). Conformational transition of initiation factor 2 from the GTP- to GDP-bound state visualized on the ribosome. *Nature Structural & Molecular Biology*, *12*(12), 1145–1149. https://doi.org/10.1038/nsmb1012

Noel, J. K., & Whitford, P. C. (2016). How EF-Tu can contribute to efficient proofreading of aa-tRNA by the ribosome. *Nature Communications*, *7*, 13314. https://doi.org/10.1038/ncomms13314

Nogales, E. (2016). The development of cryo-EM into a mainstream structural biology technique. *Nature Methods*, *13*(1), 24–27. https://doi.org/10.1038/nmeth.3694

Noller, H. F., Lancaster, L., Zhou, J., & Mohan, S. (2017). The ribosome moves: RNA mechanics and translocation. *Nature Structural & Molecular Biology*, *24*(12), 1021–1027. https://doi.org/10.1038/nsmb.3505

Ogle, J. M., Brodersen, D. E., Clemons, W. M., Jr., Tarry, M. J., Carter, A. P., & Ramakrishnan, V. (2001). Recognition of cognate transfer RNA by the 30S ribosomal subunit. *Science*, *292*(5518), 897–902. https://doi.org/10.1126/science.1060612

Ogle, J. M., & Ramakrishnan, V. (2005). Structural insights into translational fidelity. *Annual Review of Biochemistry*, *74*, 129–177. https://doi.org/10.1146/annurev.biochem.74.061903.155440

O'Reilly, F. J., Xue, L., Graziadei, A., Sinn, L., Lenz, S., Tegunov, D., Blotz, C., Singh, N., Hagen, W. J. H., Cramer, P., Stulke, J., Mahamid, J., & Rappsilber, J. (2020). In-cell architecture of an actively transcribing-translating expressome. *Science*, *369*(6503), 554–557. https://doi.org/10.1126/science.abb3758

Ou, X., Cao, J., Cheng, A., Peppelenbosch, M. P., & Pan, Q. (2019). Errors in translational decoding: tRNA wobbling or misincorporation? *PLoS Genetics*, *15*(3), e1008017. https://doi.org/10.1371/journal.pgen.1008017

Petrychenko, V., Peng, B. Z., de Schwarzer, A. C. A. P., Peske, F., Rodnina, M. V., & Fischer, N. (2021). Structural mechanism of GTPase-powered ribosome-tRNA movement. *Nature Communications*, *12*(1), 5933. https://doi.org/10.1038/s41467-021-26133-x

Polekhina, G., Thirup, S., Kjeldgaard, M., Nissen, P., Lippmann, C., & Nyborg, J. (1996). Helix unwinding in the effector region of elongation factor EF-Tu-GDP. *Structure*, *4*(10), 1141–1151. https://doi.org/10.1016/s0969-2126(96)00122-0

Prabhakar, A., Puglisi, E. V., & Puglisi, J. D. (2019). Single-molecule fluorescence applied to translation. *Cold Spring Harbor Perspectives in Biology*, *11*(1), a032714. https://doi.org/10.1101/cshperspect.a032714

Punjani, A., Rubinstein, J. L., Fleet, D. J., & Brubaker, M. A. (2017). CryoSPARC: algorithms for rapid unsupervised cryo-EM structure determination. *Nature Methods*, *14*(3), 290–296. https://doi.org/10.1038/nmeth.4169

Ramakrishnan, V. (2002). Ribosome structure and the mechanism of translation. *Cell*, *108*(4), 557–572. https://doi.org/10.1016/s0092-8674(02)00619-0

Ramrath, D. J., Lancaster, L., Sprink, T., Mielke, T., Loerke, J., Noller, H. F., & Spahn, C. M. (2013). Visualization of two transfer RNAs trapped in transit during elongation factor G-mediated translocation. *Proceedings of the National Academy of Sciences of the United States of America*, *110*(52), 20964–20969. https://doi.org/10.1073/pnas.1320387110

Ranjan, N., Pochopien, A. A., Chih-Chien Wu, C., Beckert, B., Blanchet, S., Green, R., Rodnina, M. V., & Wilson, D. N. (2021). Yeast translation elongation factor eEF3 promotes late stages of tRNA translocation. *The EMBO Journal*, *40*(6), e106449. https://doi.org/10.15252/embj.2020106449

Ratje, A. H., Loerke, J., Mikolajka, A., Brunner, M., Hildebrand, P. W., Starosta, A. L., Donhofer, A., Connell, S. R., Fucini, P., Mielke, T., Whitford, P. C., Onuchic, J. N., Yu, Y., Sanbonmatsu, K. Y., Hartmann, R. K., Penczek, P. A., Wilson, D. N., & Spahn, C. M. (2010). Head swivel on the ribosome facilitates translocation by means of intra-subunit tRNA hybrid sites. *Nature*, *468*(7324), 713–716. https://doi.org/10.1038/nature09547

Rodnina, M. V. (2018). Translation in Prokaryotes. *Cold Spring Harbor Perspectives in Biology*, *10*(9), a032664. https://doi.org/10.1101/cshperspect.a032664

Rodnina, M. V., Fischer, N., Maracci, C., & Stark, H. (2017). Ribosome dynamics during decoding. *Philosophical Transactions of the Royal Society of London. Series B, Biological Sciences*, *372*(1716), 20160182. https://doi.org/10.1098/rstb.2016.0182

Rodnina, M. V., Peske, F., Peng, B. Z., Belardinelli, R., & Wintermeyer, W. (2019). Converting GTP hydrolysis into motion: versatile translational elongation factor G. *Biological Chemistry*, *401*(1), 131–142. https://doi.org/10.1515/hsz-2019-0313

Rodnina, M. V., Savelsbergh, A., Katunin, V. I., & Wintermeyer, W. (1997). Hydrolysis of GTP by elongation factor G drives tRNA movement on the ribosome. *Nature*, *385*(6611), 37–41. https://doi.org/10.1038/385037a0

Rundlet, E. J., Holm, M., Schacherl, M., Natchiar, S. K., Altman, R. B., Spahn, C. M. T., Myasnikov, A. G., & Blanchard, S. C. (2021). Structural basis of early translocation events on the ribosome. *Nature*, *595*(7869), 741–745. https://doi.org/10.1038/s41586-021-03713-x

Salsi, E., Farah, E., Netter, Z., Dann, J., & Ermolenko, D. N. (2015). Movement of elongation factor G between compact and extended conformations. *Journal of Molecular Biology*, *427*(2), 454–467. https://doi.org/10.1016/j.jmb.2014.11.010

Samatova, E., Daberger, J., Liutkute, M., & Rodnina, M. V. (2020). Translational control by ribosome pausing in bacteria: How a non-uniform pace of translation affects protein production and folding. *Frontiers in Microbiology*, *11*, 619430. https://doi.org/10.3389/fmicb.2020.619430

Santos, N., Zhu, J., Donohue, J. P., Korostelev, A. A., & Noller, H. F. (2013). Crystal structure of the 70S ribosome bound with the Q253P mutant form of release factor RF2. *Structure*, *21*(7), 1258–1263. https://doi.org/10.1016/j.str.2013.04.028

Scheres, S. H. (2012). RELION: implementation of a Bayesian approach to cryo-EM structure determination. *Journal of Structural Biology*, *180*(3), 519–530. https://doi.org/10.1016/j.jsb.2012.09.006

Schmeing, T. M., Voorhees, R. M., Kelley, A. C., Gao, Y. G., Murphy, F. V., Weir, J. R., & Ramakrishnan, V. (2009). The crystal structure of the ribosome bound to EF-Tu and aminoacyl-tRNA. *Science*, *326*(5953), 688–694. https://doi.org/10.1126/science.1179700

Sharma, H., Adio, S., Senyushkina, T., Belardinelli, R., Peske, F., & Rodnina, M. V. (2016). Kinetics of spontaneous and EF-G-accelerated rotation of ribosomal subunits. *Cell Reports*, *16*(8), 2187–2196. https://doi.org/10.1016/j.celrep.2016.07.051

Shin, D. H., Brandsen, J., Jancarik, J., Yokota, H., Kim, R., & Kim, S. H. (2004). Structural analyses of peptide release factor 1 from *Thermotoga maritima* reveal domain flexibility required for its interaction with the ribosome. *Journal of Molecular Biology*, *341*(1), 227–239. https://doi.org/10.1016/j.jmb.2004.05.055

Shine, J., & Dalgarno, L. (1974). The 3′-terminal sequence of *Escherichia coli* 16S ribosomal RNA: complementarity to nonsense triplets and ribosome binding sites. *Proceedings of the National Academy of Sciences of the United States of America*, *71*(4), 1342–1346. https://doi.org/10.1073/pnas.71.4.1342

Simonetti, A., Marzi, S., Billas, I. M., Tsai, A., Fabbretti, A., Myasnikov, A. G., Roblin, P., Vaiana, A. C., Hazemann, I., Eiler, D., Steitz, T. A., Puglisi, J. D., Gualerzi, C. O., & Klaholz, B. P. (2013). Involvement of protein IF2 N domain in ribosomal subunit joining revealed from architecture and function of the full-length initiation factor. *Proceedings of the National Academy of Sciences of the United States of America*, *110*(39), 15656–15661. https://doi.org/10.1073/pnas.1309578110

Simonetti, A., Marzi, S., Myasnikov, A. G., Fabbretti, A., Yusupov, M., Gualerzi, C. O., & Klaholz, B. P. (2008). Structure of the 30S translation initiation complex. *Nature*, *455*(7211), 416–420. https://doi.org/10.1038/nature07192

Sprink, T., Ramrath, D. J., Yamamoto, H., Yamamoto, K., Loerke, J., Ismer, J., Hildebrand, P. W., Scheerer, P., Burger, J., Mielke, T., & Spahn, C. M. (2016). Structures of ribosome-bound initiation factor 2 reveal the mechanism of subunit association. *Science Advances*, *2*(3), e1501502. https://doi.org/10.1126/sciadv.1501502

Steitz, J. A., & Jakes, K. (1975). How ribosomes select initiator regions in mRNA: base pair formation between the 3′ terminus of 16S rRNA and the mRNA during initiation of protein synthesis in *Escherichia coli*. *Proceedings of the National Academy of Sciences of the United States of America*, *72*(12), 4734–4738. https://doi.org/10.1073/pnas.72.12.4734

Svidritskiy, E., Demo, G., Loveland, A. B., Xu, C., & Korostelev, A. A. (2019). Extensive ribosome and RF2 rearrangements during translation termination. *eLife*, *8*, e46850. https://doi.org/10.7554/eLife.46850

Svidritskiy, E., & Korostelev, A. A. (2018). Conformational control of translation termination on the 70S ribosome. *Structure*, *26*(6), 821–828. https://doi.org/10.1016/j.str.2018.04.001

Tang, G., Peng, L., Baldwin, P. R., Mann, D. S., Jiang, W., Rees, I., & Ludtke, S. J. (2007). EMAN2: an extensible image processing suite for electron microscopy. *Journal of Structural Biology*, *157*(1), 38–46. https://doi.org/10.1016/j.jsb.2006.05.009

Trappl, K., & Joseph, S. (2016). Ribosome induces a closed to open conformational change in release factor 1. *Journal of Molecular Biology*, *428*(6), 1333–1344. https://doi.org/10.1016/j.jmb.2016.01.021

Vestergaard, B., Van, L. B., Andersen, G. R., Nyborg, J., Buckingham, R. H., & Kjeldgaard, M. (2001). Bacterial polypeptide release factor RF2 is structurally distinct from eukaryotic eRF1. *Molecular Cell*, *8*(6), 1375–1382. https://doi.org/10.1016/s1097-2765(01)00415-4

Voorhees, R. M., Schmeing, T. M., Kelley, A. C., & Ramakrishnan, V. (2010). The mechanism for activation of GTP hydrolysis on the ribosome. *Science*, *330*(6005), 835–838. https://doi.org/10.1126/science.1194460

Wang, C., Molodtsov, V., Firlar, E., Kaelber, J. T., Blaha, G., Su, M., & Ebright, R. H. (2020). Structural basis of transcription-translation coupling. *Science*, *369*(6509), 1359–1365. https://doi.org/10.1126/science.abb5317

Warias, M., Grubmuller, H., & Bock, L. V. (2020). tRNA dissociation from EF-Tu after GTP hydrolysis: Primary steps and antibiotic inhibition. *Biophysical Journal*, *118*(1), 151–161. https://doi.org/10.1016/j.bpj.2019.10.028

Wasserman, M. R., Alejo, J. L., Altman, R. B., & Blanchard, S. C. (2016). Multiperspective smFRET reveals rate-determining late intermediates of ribosomal translocation. *Nature Structural & Molecular Biology*, *23*(4), 333–341. https://doi.org/10.1038/nsmb.3177

Webster, M. W., Takacs, M., Zhu, C., Vidmar, V., Eduljee, A., Abdelkareem, M., & Weixlbaumer, A. (2020). Structural basis of transcription-translation coupling and collision in bacteria. *Science*, *369*(6509), 1355–1359. https://doi.org/10.1126/science.abb5036

Weissenberger, G., Henderikx, R. J. M., & Peters, P. J. (2021). Understanding the invisible hands of sample preparation for cryo-EM. *Nature Methods*, *18*(5), 463–471. https://doi.org/10.1038/s41592-021-01130-6

Weixlbaumer, A., Jin, H., Neubauer, C., Voorhees, R. M., Petry, S., Kelley, A. C., & Ramakrishnan, V. (2008). Insights into translational termination from the structure of RF2 bound to the ribosome. *Science*, *322*(5903), 953–956. https://doi.org/10.1126/science.1164840

Wilden, B., Savelsbergh, A., Rodnina, M. V., & Wintermeyer, W. (2006). Role and timing of GTP binding and hydrolysis during EF-G-dependent tRNA translocation on the ribosome. *Proceedings of the National Academy of Sciences of the United States of America*, *103*(37), 13670–13675. https://doi.org/10.1073/pnas.0606099103

Wohlgemuth, I., Pohl, C., & Rodnina, M. V. (2010). Optimization of speed and accuracy of decoding in translation. *The EMBO Journal*, *29*(21), 3701–3709. https://doi.org/10.1038/emboj.2010.229

Yamane, T., Miller, D. L., & Hopfield, J. J. (1981). Discrimination between D- and L-tyrosyl transfer ribonucleic acids in peptide chain elongation. *Biochemistry*, *20*(25), 7059–7064. https://doi.org/10.1021/bi00528a001

Yi, S. H., Petrychenko, V., Schliep, J. E., Goyal, A., Linden, A., Chari, A., Urlaub, H., Stark, H., Rodnina, M. V., Adio, S., & Fischer, N. (2022). Conformational rearrangements upon start codon recognition in human 48S translation initiation complex. *Nucleic Acids Research*, *50*(9), 5282–5298. https://doi.org/10.1093/nar/gkac283

Zhang, J., Ieong, K. W., Johansson, M., & Ehrenberg, M. (2015). Accuracy of initial codon selection by aminoacyl-tRNAs on the mRNA-programmed bacterial ribosome. *Proceedings of the National Academy of Sciences of the United States of America*, *112*(31), 9602–9607. https://doi.org/10.1073/pnas.1506823112

Zheng, S. Q., Palovcak, E., Armache, J. P., Verba, K. A., Cheng, Y., & Agard, D. A. (2017). MotionCor2: anisotropic correction of beam-induced motion for improved cryo-electron microscopy. *Nature Methods*, *14*(4), 331–332. https://doi.org/10.1038/nmeth.4193

Zhou, J., Lancaster, L., Donohue, J. P., & Noller, H. F. (2013). Crystal structures of EF-G-ribosome complexes trapped in intermediate states of translocation. *Science*, *340*(6140), 1236086. https://doi.org/10.1126/science.1236086

Zivanov, J., Nakane, T., Forsberg, B. O., Kimanius, D., Hagen, W. J., Lindahl, E., & Scheres, S. H. (2018). New tools for automated high-resolution cryo-EM structure determination in RELION-3. *eLife*, *7*, e42166. https://doi.org/10.7554/eLife.42166

How to cite this article: Zafar, H., Hassan, A. H., & Demo, G. (2023). Translation machinery captured in motion. *WIREs RNA*, e1792. https://doi.org/10.1002/wrna.1792